Structure and Properties of Ti/TiB Metal–Matrix Composite after Isothermal Multiaxial Forging

S. Zherebtsov[*], M. Ozerov, N. Stepanov and M. Klimova

Belgorod State University, Pobeda-85, Belgorod 308015, Russia

Microstructure and mechanical properties of a Ti/TiB metal–matrix composites after multiaxial forging at 850 °C to the true strain $\varepsilon = 5.2$ were studied. The composite with 17 vol.% of TiB was produced via spark plasma sintering at 1000 °C. Mechanical behavior in terms of aggregated σ-$\Sigma\varepsilon$ curves during the multiaxial forging demonstrated a pronounced softening following by a steady-like flow stage. The length of TiB whiskers considerably decreased after the first step of the multiaxial forging and then changed insignificantly. The microstructure after the MAF consisted of dislocation-free Ti matrix areas of ≈ 1 μm in diameter and areas with high density of TiB whiskers and high dislocation density. The forging resulted in a considerable increase in ductility of the Ti/TiB metal–matrix composites at room and elevated temperatures without loss in strength.

1. Introduction

One of the attractive way to increase strength-related properties (strength, hardness, wear resistance, etc.) in titanium and low-alloyed titanium alloys is associated with creating Ti matrix composites with embedded ceramic reinforcements by, for example, spark plasma sintering (SPS) technology [1–3]. Among various reinforcements TiB has a close to titanium density, it creates minimal residual stresses and has good crystallographic interface with the Ti matrix [4, 5]. During the SPS the TiB whiskers form as a result of the chemical reaction Ti+TiB$_2$ =Ti+2TiB. However, along with the increased strength, Ti/TiB metal–matrix composites (MMCs) demonstrate poor low-temperature ductility. Mechanical properties of the MMCs can be improved by thermo-mechanical treatment, for example multiple isothermal 2D forging (drawing) [6, 7]. In this paper, microstructure and mechanical properties of 17 vol.% TiB reinforced titanium matrix composites produced by SPS at 1000 °C was studied after multiaxial forging at 850 °C to $\varepsilon = 5.2$.

2. Materials and procedure

Commercial Ti and TiB$_2$ powders of ≈ 25 and ≈ 4 μm in diameter, respectively, were used as the raw materials. A mixture of 90 wt% Ti and 10 wt% TiB$_2$ (which yields 17 vol.% of TiB during the reaction of Ti + TiB$_2$ → Ti + 2TiB [8]) was prepared using a Retsch RS 200 vibrating cup mill for 1 h in ethanol at the milling rotation speed of 700 rpm.

Ti/TiB MMC specimens measuring 15 mm in height and 19 mm in diameter were produced using the SPS process under vacuum on a Thermal Technology SPS 10-3 machine at 1000 °C and 40 MPa for 15 min.

The specimens were subjected to multiaxial forging (MAF) which comprised successive compressions of a sample along three orthogonal directions (this method is also known as "abc" deformation [9]). The initial strain rate and the true strain per deformation step were 10^{-3}/s and ≈ 0.5, respectively. Compressions were performed on an Instron 300LX testing machine in air at 850 °C. Stress–strain curves were recorded for each step. Ten compressions in total were made (the true cumulative strain $\Sigma\varepsilon \approx 5.2$).

A JEOL JEM-2100 transmission electron microscope (TEM) and a Quanta 600 FEG (field-emission-gun) scanning-electron microscope (SEM) were used for microstructure examination of the central region of the specimens. SEM specimens were etched using Kroll's reagent (95% H$_2$O, 3% HNO$_3$, 2% HF)

Tensile or compression tests were conducted on an Instron 5882 testing machine at 300 °C, 400 °C, and 500 °C (tensile) or room temperature (compression) at an initial strain rate of 10^{-3}/s. The tensile samples had the gauge measuring 4 mm length and 3 mm×1.5 mm cross-section. The compression specimens were measured as $6 \times 4 \times 4$ mm^3. Both the compression and tensile tests were carried out without extensometer mainly due to a very small gage size of the specimens.

3. Results and discussion

In the initial (as-sintered) condition the microstructure of the MMC consisted of TiB whiskers with the average diameter 63±35 nm heterogeneously distributed within the Ti matrix (Fig. 1). In the majority of the microstructure a very high dislocation density was observed most probably due to a large number of TiB particles. Some unreacted TiB$_2$ particles (the volume fraction of 2%) were observed in the microstructure. The residual porosity was $\approx 0.5\%$.

True stress–true strain curves obtained during multiaxial isothermal forging at 850 °C showed an initial hard-

———————

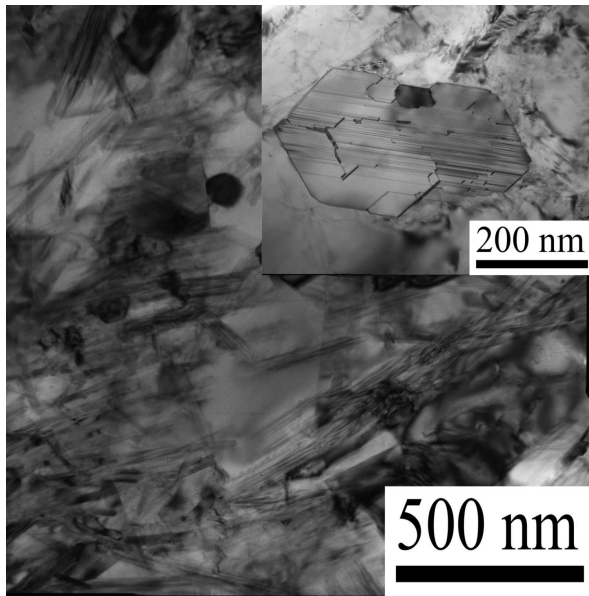[*]corresponding author; e-mail: ser_z@mail.ru

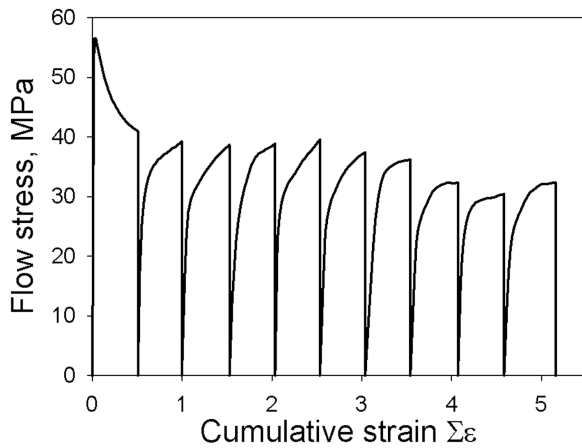Fig. 1. Bright-field TEM image of Ti/TiB MMC microstructure; the inset shows a cross-section of a TiB whisker.

Fig. 2. True stress–true strain curves obtained during the MAF at $850\,^{\circ}$C.

Fig. 3. SEM (a) and TEM bright-field (b) images of the Ti/TiB composite after the MAF at $850\,^{\circ}$C to $e = 5.2$ (10 steps).

ening transient, a peak flow stress, and then flow softening during the first compression (Fig. 2). However at late stages ($\Sigma e > 3$) each stress–strain curve demonstrated a steady-state-like behavior after initial hardening. A noticeable difference between the flow stresses in the end of each step and the yield stress of the next step was observed. It should be noted also that the flow stress had a trend to decrease with increase of cumulative strain.

Microstructure of the Ti/TiB metal–matrix composite changed considerably as a result of the MAF. A lot of small fragments of TiB were observed in the microstructure of the strained condition (Fig. 3a).

Meanwhile TEM analysis showed that deformation at $850\,^{\circ}$C to $e = 5.2$ (10 steps) resulted in the formation of separate areas (1–1.5 μm in diameter) with a much lower dislocation density compared with the neighbor-
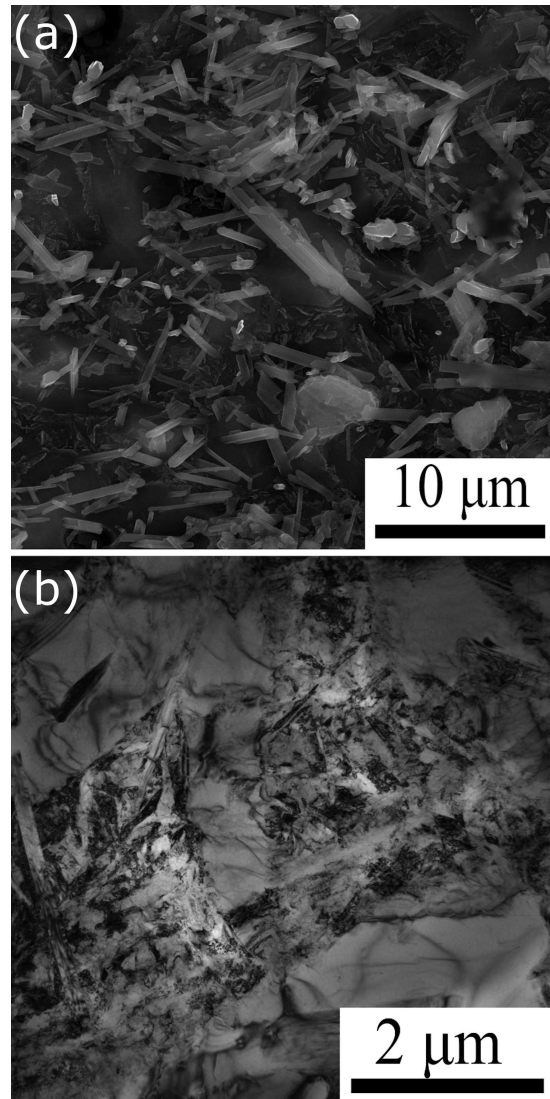
ing fields (Fig. 3b). The estimated dislocation density in these areas was $\approx 2 \times 10^{12}$ m^{-2}. The boundaries of some dislocation-free areas can be well-defined. The development of recovery or recrystallization was more evident in the areas of the Ti matrix with a relatively low density of the TiB whiskers. The greater density of the TiB particles most likely hindered grain boundary movement thereby preserving the microstructure with a high dislocation density.

Quantitative analysis showed that the diameter of the whiskers did not noticeably change during the MAF. The apparent length of whiskers decreased considerably, by a factor of ≈ 3, after the first step of the MAF and then remained almost unchanged during further deformation (Fig. 4). Thus, the length-to-diameter aspect ratio of TiB whiskers approached stable value (≈ 10) at the initial stages of deformation and had not changed further.
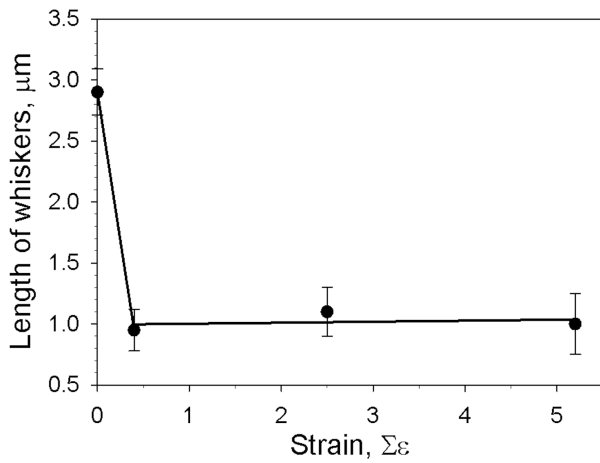
Fig. 4. Apparent length of TiB whiskers in Ti/TiB MMCs during the MAF.

Mechanical behavior of the MMCs obtained in compression at room temperature (Fig. 5a) or in tension at 300–500 °C (Fig. 5b) showed considerable improvement of ductility of the specimens after the MAF to $e = 5.2$ (10 steps) at 850 °C. The samples of the MMC after the MAF at 850 °C demonstrated noticeable compression ductility ($\approx$ 2–3%) at room temperature and similar tensile ductility at 300 °C. Meanwhile in the as-sintered condition the tensile specimen of MMC fractured just after the elastic region even at 400 °C. Some tensile elongation of the as-sintered composite was recorded only at 500 °C. The ultimate compression strength of the forged and as-sintered specimens was quite similar at room temperature (2210 and 1960 MPa, respectively) while at elevated temperatures the specimens after the MAF became noticeably stronger. Quite a large stage of elasticity observed in all conditions of the MMC can be associated with the conducting of the tensile test without extensometer; in this case elastic deformation of the tensile machine parts was also included into the overall elastic deformation shown in the stress–strain diagram. In addition the Young modulus of the composite is not too high ($\approx$ 200 GPa [4, 10]) while the yield stress at room temperature almost attained 2000 MPa.

After the MAF the ultimate strengths were found to be 765 MPa at 300 °C and 540 MPa at 400 °C while in the as-sintered condition the maximum attained strengths were 480 MPa at 400 °C and 520 MPa at 500 °C.

Therefore the results obtained in the current study show a possibility to increase considerably low-temperature ductility without loss in strength of the Ti/TiB MMCs by the multiaxial isothermal forging at 850 °C to ε =5.2. The observed improvement of the mechanical properties is most likely associated with the microstructure developed during the MAF. One of the most obvious effects of plastic deformation at elevated temperatures on the microstructure of Ti/TiB MMC was a considerable (by $\approx$ 3 times) decrease in the length of the TiB whiskers. This change occurred in the very beginning of
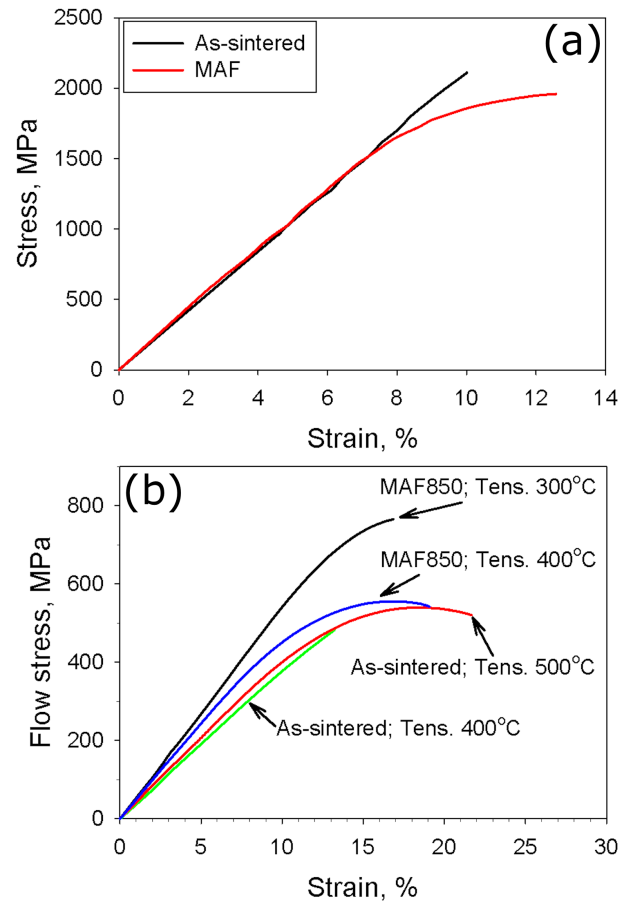

Fig. 5. Stress–strain curves of Ti/TiB MMC in different conditions tested in compression at room temperature (a) or in tension at elevated temperatures (b).

the MAF (Fig. 4) causing, most likely, the corresponding decrease in the flow stress after the first compression (Fig. 2). Since the apparent length of the TiB whiskers did not decrease noticeably with further strain, a stable aspect ratio of $\approx$ 10 was achieved. The aspect ratio of the TiB (rather than the diameter) is considered to be the main factor that influences the mechanical properties of the MMCs. It was shown in [11] that whiskers with a large value of aspect ratio make a greater contribution to the strength of the composite. In turn this can be associated with different contribution of various strengthening mechanisms (mainly the Orowan mechanism or hardening due to a load transfer from the Ti matrix to TiB by an interfacial shear stress [12]) depending on the length-to-diameter ratio. Therefore a stable length-to-diameter ratio after the MAF can result in the observed improvement of strength and ductility in comparison with the as-sintered condition (Fig. 5).

Some difference in the mechanical properties of the MMC after the MAF can also be ascribed to the structure of the Ti matrix. The development of discontinuous dynamic recrystallization in the Ti matrix of the MMC can be proved by the formation of dislocation-free areas

(Fig. 3b) and characteristic type of the aggregated mechanical behavior with a steady-like flow stage during the MAF at 850 °C (Fig. 2) [13] and agrees with the previous data [3]. It is known that the presence of recrystallized areas in nanostructured materials enhance their strain hardening capacity and thus promote ductility [14]. In the studied Ti/TiB composite, the combination of the recrystallized Ti grains and the areas with high dislocation density strengthened by the nanosized TiB whiskers provides a good balance of strength and ductility which exceeds the corresponding properties of the as-sintered material.

4. Conclusions

1. Mechanical behavior during the MAF at 850 °C can be described by an aggregated σ–$\Sigma\varepsilon$ curves which demonstrated a pronounced softening following by a steady-like state flow. The observed mechanical behavior can be associated with the formation of a stable aspect ratio of ≈ 10 of the TiB whiskers during the MAF and development of discontinuous dynamic recrystallization. The MAF resulted in the formation of a homogeneous microstructure with dislocation-free areas of ≈ 1 μm and areas with high density of TiB and high dislocation density.

2. The MAF at 850 °C to cumulative strain ≈ 5.2 resulted in a considerable increase in low-temperature ductility without loss in strength. For instance, nearly zero ductility was obtained in the as-sintered specimen during compression at room temperature, whereas specimens after the MAF demonstrated at this temperature $\approx 3\%$ ductility.

Acknowledgments

References

[1] T. Saito, T. Furuta, T. Yamaguchi, in: *Recent Advances in Titanium Metal Matrix Composites*, Eds. F.H. Froes, J. Storer, The Minerals, Metals and Materials Society, Warrendale 1995, p. 33.

[2] L.J. Huang, L. Geng, H-X. Peng, *Prog. Mater. Sci.* **71**, 93 (2015).

[3] M. Ozerov, M. Klimova, A. Kolesnikov, N. Stepanov, S. Zherebtsov, *Mater. Des.* **112,** 17 (2016).

[4] K. Morsi, V.V. Patel, *J. Mater. Sci.* **42**, 2037 (2007).

[5] H. Feng, Y. Zhou, D. Jia, Q. Meng, J. Rao, *Cryst. Growth Des.* **6**, 1626 (2006).

[6] R.A. Gaisin, V.M. Imayev, R.M. Imayev, *J. Alloys Comp.* **723**, 385 (2017).

[7] V. Imayev, R. Gaisin, E. Gaisina, R. Imayev, H.-J. Fecht, F. Pyczak, *Mater. Sci. Eng. A Struct.* **609**, 34 (2014).

[8] L.J. Huang, L. Geng, B. Wang, L.Z. Wu, *Mater. Des.* **45**, 532 (2013).

[9] G.A. Salishchev, S.Yu. Mironov, S.V. Zherebtsov, *Rev. Adv. Mater. Sci.* **11**, 152 (2006).

[10] K.S. Ravi Chandran, K.B. Panda, S.S. Sahay, *JOM* **56**, 42 (2004).

[11] M.Y. Koo, J.S. Park, M.K. Park, K.T. Kim, S.H. Hong, *Scr. Mater.* **66**, 487 (2012).

[12] B. Chen, J. Shen, X. Ye, L. Jia, S. Li, J. Umeda, M. Takahashi, K. Kondoh, *Acta Mater.* **140**, 317 (2017).

[13] F. Humphreys, M. Hatherly, *Recrystallization and Related Annealing Phenomena*, Elsevier, Oxford 2004.

[14] Y. Wang, M. Cheng, F. Zhou, E. Ma, *Nature* **419**, 912 (2002).